Single particle damage events in candidate star camera sensors

Paul Marshall[1], Cheryl Marshall[2], Elizabeth Polidan[3], Augustyn Wacyznski[3] and Scott Johnson[3]

1 NASA GSFC Consultant,
2 NASA GSFC
3 Global Science and Technology, NASA-GSFC

Abstract

Si charge coupled devices (CCDs) are currently the preeminent detector in star cameras as well as in the near ultraviolet (UV) to visible wavelength region for astronomical observations in space and in earth-observing space missions. Unfortunately, the performance of CCDs is permanently degraded by total ionizing dose (TID) and displacement damage effects. TID produces threshold voltage shifts on the CCD gates and displacement damage reduces the charge transfer efficiency (CTE), increases the dark current, produces dark current nonuniformities and creates random telegraph noise in individual pixels. In addition to these long term effects, cosmic ray and trapped proton transients also interfere with device operation on orbit. In the present paper, we investigate the dark current behavior of CCDs – in particular the formation and annealing of hot pixels. Such pixels degrade the ability of a CCD to perform science and also can present problems to the performance of star camera functions (especially if their numbers are not correctly anticipated).

To date, most dark current radiation studies have been performed by irradiating the CCDs at room temperature but this can result in a significantly optimistic picture of the hot pixel count. We know from the Hubble Space Telescope (HST) that high dark current pixels (so-called hot pixels or hot spikes) accumulate as a function of time on orbit [1,2]. For example, the HST Advanced Camera for Surveys/Wide Field Camera instrument performs monthly anneals despite the loss of observational time, in order to partially anneal the hot pixels. Note that the fact that significant reduction in hot pixel populations occurs for room temperature anneals is not presently understood since none of the commonly expected defects in Si (e.g. divacancy, E center, and A-center) anneal at such a low temperature.

A HST Wide Field Camera 3 (WFC3) CCD manufactured by E2V was irradiated while operating at -83 °C and the dark current studied as a function of temperature while the CCD was warmed to a sequence of temperatures up to a maximum of +30°C. The device was then cooled back down to -83° and re-measured. Hot pixel populations were tracked during the warm-up and cool-down. Hot pixel annealing began below -40 °C and the anneal process was largely completed before the detector reached +30°C. There was no apparent sharp temperature dependence in the annealing. Although a large fraction of the hot pixels fell below the threshold to be counted as a hot pixel, they nevertheless remained warmer than the remaining population. The details of the mechanism for the formation and annealing of hot pixels is not presently understood, but it appears likely that hot pixels are associated with displacement damage occurring in high electric field regions.

Single particle damage events in candidate star camera sensors

Paul Marshall[1], Cheryl Marshall[2], Elizabeth Polidan[3], Augustyn Wacyznski[3] and Scott Johnson[3]

1 NASA GSFC Consultant,
2 NASA GSFC
3 Global Science and Technology, NASA-GSFC

Si charge coupled devices (CCDs) are currently the preeminent detector in star cameras as well as in the near ultraviolet (UV) to visible wavelength region for astronomical observations in space and in earth-observing space missions. Specialized scientific CCDs have also been developed for use in the UV and x-ray regimes. Many science and star tracking functions have been performed using CCDs despite their well-known vulnerability to radiation damage. Although other visible technologies such as active pixel sensor (APS) arrays offer some advantages with respect to radiation hardness, suitably low-noise APS devices are not presently commercially available.

The performance of CCDs and APS devices is permanently degraded by total ionizing dose (TID) and displacement damage effects[1]. TID damages oxides resulting in threshold voltage shifts on the CCD gates and can increase the dark current from both bulk displacement damage from particle collisions with Si lattice atoms and from ionization damage and surface state formation in non-multiphase pinned (MPP) devices. Especially for missions with requirements less than about 10 krads(Si), the TID-induced radiation response can generally be managed. However, it is important to verify that flatband shifts will not take a device out of inversion prior to the expected mission dose, and also to ensure that the readout amplifier circuitry is robust.

This paper will focus on displacement damage which reduces the charge transfer efficiency (CTE) of a CCD and increases the average dark current as well as dark current nonuniformity. Displacement damage is produced by energetic particles such as protons and neutrons which collide with silicon atoms and displace them from their lattice sites. As a result many vacancy interstitial pairs are formed, most of which recombine with no permanent change in electrical properties. The vacancies that survive migrate in the lattice and form stable defects such as the phosphorus-vacancy complex (or E-center), oxygen-vacancy defect (or A-center), divacancy, etc. These defects degrade CCD performance by decreasing the CTE due to the introduction of electron traps, and increasing the average dark current and dark current nonuniformity by introducing individual pixels with very high dark currents ("hot pixels" or "spikes"), and by introducing random telegraph noise in pixels[1]. In addition to these long term effects, cosmic ray and trapped proton transients also interfere with device operation on orbit.

Depending on the specific application, star tracker performance can be limited by either CTE or dark current degradation. In star camera applications, these degrading effects show up in as error terms that result in systematic bore sight misalignment and increased noise equivalent aperture. In addition, some applications require the identification of hot pixels and associated processing complexity to reject position information when tracked stars encounter excessively

high dark current pixels. In this paper we will emphasize the role hot pixel (or "spike") production as a degradation mode for any sensor array, be it CCD, charge injection device (CID), APS, or Si hybrid devices. To do this, we examine how the production of hot pixels is governed by the collision kinematics and electric field distributions in the pixel volumes, and also consider the annealing of hot pixels and how operating temperature affects this.

Proton induced displacement damage on CCDs increases the dark current as a result of carrier generation in the bulk depletion region of the pixel. (This assumes that the CCD has a hardened oxide and/or else is run in inversion so that the surface dark current is suppressed.) The average dark current increase has been shown to correlate with the amount of displacement damage energy imparted to the Si lattice by incoming protons.[2] Note that on average the lower energy protons are more damaging than high energy protons. Although the increase in the mean dark current with proton irradiation is important, the dark current nonuniformity is often the biggest concern for imager applications in space. Much of this nonuniformity is inherent to the statistical nature of the collision kinematics producing the displacement damage and therefore cannot be hardened against. Incoming protons of the same energy may produce very different amounts of displacement damage depending on the particular collision sequence that follows as illustrated in Figure 1.[3] This is an inherent property of the collision process and cannot be avoided. Very large dark current pixels can be produced when a collision occurs in a high electric field region (e.g. > 10^5 volts/cm) of a pixel as a result of electric field enhanced emission. (See reference 3 and references therein for more details.) Such hot pixels have been observed in CIDs as just described but also in CCDs[4] and APS[5] devices.

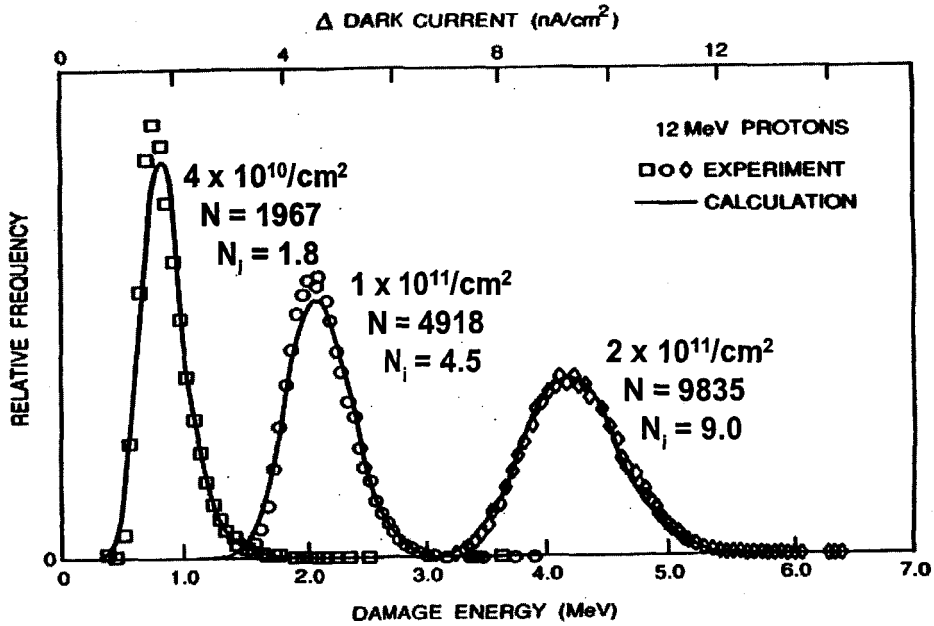

Figure 1 Charge Injection Device (CID) dark current histograms after exposure of a 256x256 array to increasing fluences of 12 MeV protons. After [3]. N is the average number of coulombic scattering events, and note as the number of primary proton-Si interactions per pixel increases, the distribution approaches a gaussian distribution. This shape, and the high energy tail are consequences of very infrequent but large nuclear reaction events. (N_i is the average number of inelastic interactions per pixel.) Such dark current nonuniformities are observed for any array of identical pixels whether it be a CID, CCD or APS device.

High dark current pixels (so-called hot pixels or spikes) accumulate as a function of time on orbit and present a serious problem for some missions. For example, the HST ACS/WFC instrument performs monthly anneals from the operating temperature of -83°C to around room temperature despite the loss of observational time, in order to partially anneal the hot pixels as demonstrated in figure 2.[6] Note that the fact that significant annealing occurs for room temperature anneals is not presently understood since none of the commonly expected defects in Si (e.g. divacancy, E-center, and A-center) anneal at such a low temperature.

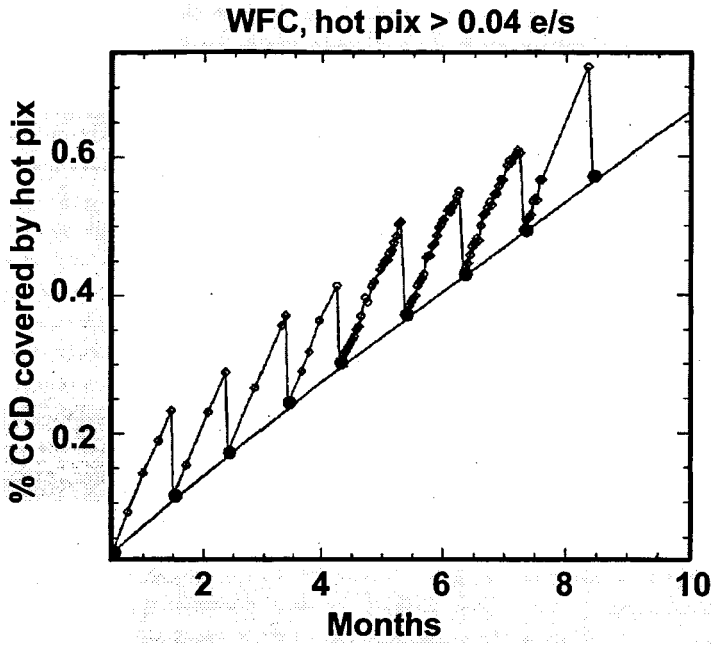

Figure 2. Hot pixel growth rates require monthly anneals that consume 10% of the observing time on the HST instruments (STIS, WFC2, ACS). From [6].

THE EXPERIMENT

The HST Wide Field Camera 3 (WFC3) CCDs are 2048x4096 CCD43s manufactured by E2V with a 15 μm square pixel, a supplemental buried channel, a multi-phase pinned (MPP) implant, and are backside illuminated. This device was operated with a read noise of ~ 3 electrons RMS, and is in many ways similar to CCDs used in star camera applications, with the exception that it was read in full frame mode and all pixels were read in each acquisition sequence. The device was irradiated at the University of California at Davis cyclotron while operating at -83 °C using a dewar specifically designed for proton irradiations. After the CCD was exposed to <1 x 10^3 cm^{-2} 63 MeV protons for alignment purposes, it was further irradiated in steps ranging from 8.33 x 10^7 cm^{-2} to 2.25 x 10^9 cm^{-2} which corresponds to 1 month and 27 months, respectively of time in the HST orbit. The correspondence between 63 MeV proton fluence and orbital exposure is based on the equivalence of non-ionizing energy loss rate (NIEL) damage as predicted for the HST WFC3 environment.[2] For ionizing dose, this proton energy

deposits 170 rads(Si) per 1.0 x 10^9 cm^{-2} fluence, and this is therefore in a relative light damage regime relative to many star camera applications.

Prior to irradiation, a series of exposures (with integration times appropriate to the temperature) were taken at the CCD's nominal operating temperature of -83°C as well at -40°C, -20°C, -10°C, 0°C, +10°C, +20°C and +30°C with a readout speed of 50 kHz, in MPP mode and at a frame rate of 90 s. The CCD was irradiated to 8.33 x 10^7 cm^{-2} at -83°C and the dark current distributions studied at each of the temperatures cited above. After a 4 hour soak at +30°C, the device was then cooled back down to -83°C and re-measured. This entire sequence was repeated twice more to simulate the device response to the proposed annealing schedule after the equivalent of 2 months and 3 months worth of on-orbit proton exposure. Finally, the CCD was exposed to an additional 2.25 x 10^9 cm^{-2} protons to bring the total exposure to the on-orbit equivalent of 30 months, or 2.50 x 10^9 cm^{-2}. At each step, multiple exposures were acquired to enable cosmic ray and proton-induced activation rejection. More details about the experimental set-up and data acquisition schedule may be found in.[7]

RESULTS AND DISCUSSION

Figure 3 shows the dark current distributions at -83°C before and after annealing at +30°C. Clearly significant annealing is associated with the hot pixels but there is no information concerning the fate of the pixels that were originally hot pre-anneal, but are apparently no longer hot post-anneal.

Following the techniques described in [3] the dark current distribution expected based on the collisional kinematics was calculated. It was determined that the "humps" observed on the high dark current sides of the distributions are not due to inelastic collisions. We suspect electric field enhanced emission as the cause of these hot pixels and will present activation energy data in the full paper to support this hypothesis. The mean dark currents were in line with that expected based on the damage constants reported by Srour and Lo [8].

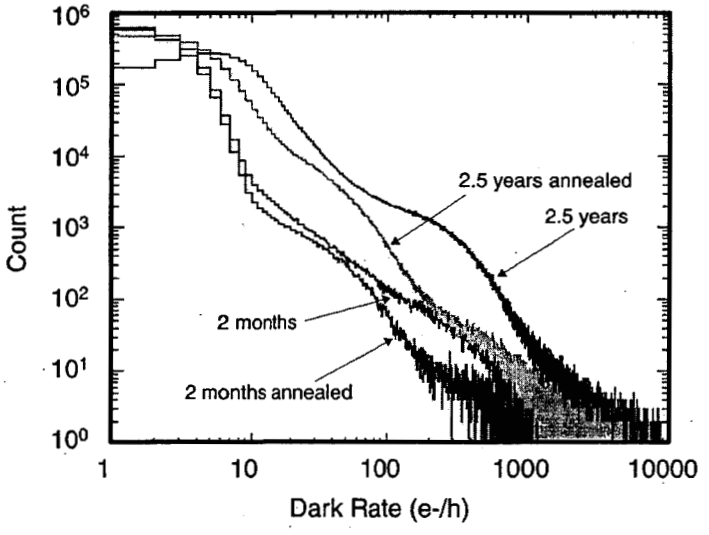

Figure 3. Comparison of dark current distributions before and after annealing at +30°C for two exposure levels. The data were acquired at -83°C and the mean pre-irradiation dark current was <0.1 e^-/pixel/hr.

Populations of hot pixels (defined as pixels having more than a given dark current threshold) were tracked to identify whether a hot pixel encountered at any step in the above-described measurement sequence is a new hot pixel or an existing one. Figure 4 shows 4 distinct hot pixel (defined as >40e⁻/pixel/hr) populations at -83°C. The threshold value of >40e⁻/pixel/hr is somewhat arbitrary and represents a value of 100 times the mean dark current in the prerad dark current histogram. The figure shows hot pixel populations corresponding to proton exposures representing the first (1 month, R1), second (cumulative 2 month, R2), third (cumulative 3 month, R3) and fourth (cumulative 27 month, R4) exposures. Note that in each post irradiation soak at +30°C (A1-A4, respectively) further annealing is observed although the bulk of the annealing is complete after the first soak at +30°C. Details of issues that arose in tracking the individual pixels will be described in the full paper. The benefit of the 4 hour soaks at +30°C is easily seen in Figure 2. The annealing rates for the hot pixels is consistent with those observed on other HST cameras.[9,10]

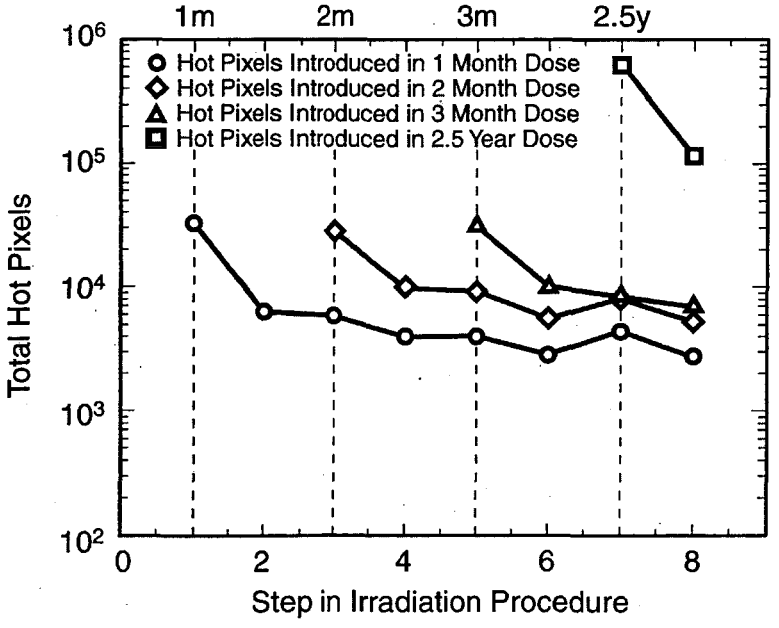

Figure 4. Four separate populations of hot pixels (defined as >40 e⁻/pixel/hr) introduced at each radiation step (R1-R4). In each case, the first anneal is always the most effective at reducing the hot pixel count.

As seen in Figure 5, the growth in the hot pixel population after annealing is linear with fluence. Similar behavior was observed for the other thresholds.

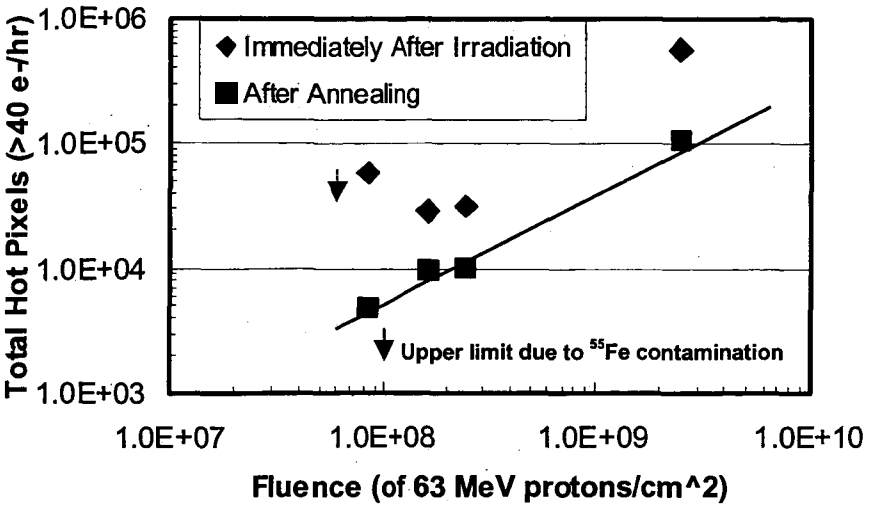

Figure 5 The total number of hot pixels (in this case defined as >40 e⁻/pixel/hr) immediately after irradiation as well as after annealing.

Figure 6 shows the number of hot pixels that annealed and had their magnitude fall below 100 x and 200 x the mean of the dark distribution. These levels were chosen because they correspond to the thresholds for the hot pixels identified at -83°C (40e⁻/pixel/hr is approximately equal to 100 x the mean dark current immediately after irradiation). Hot pixel populations were tracked during the warm-up and cool-down. It appears that the annealing process starts somewhere below -40°C and continues through warmer temperatures. Note that to the extent that hot pixels have a lower activation energy as observed in [11], we have a built-in source of false positives for annealing as we warm up. However, Figure 6 still shows that there is no sharp temperature at which annealing occurs. The plot in the figure indicates an apparent peak at 0°C, but this may be an artifact caused by the saturation of hot pixels as discussed further in [13]. Above this temperature thresholds (of 100x and 200x mean dark current) are higher than the available dynamic range, and saturating pixels were discarded so the number of non-saturated hot pixels rapidly decreases.

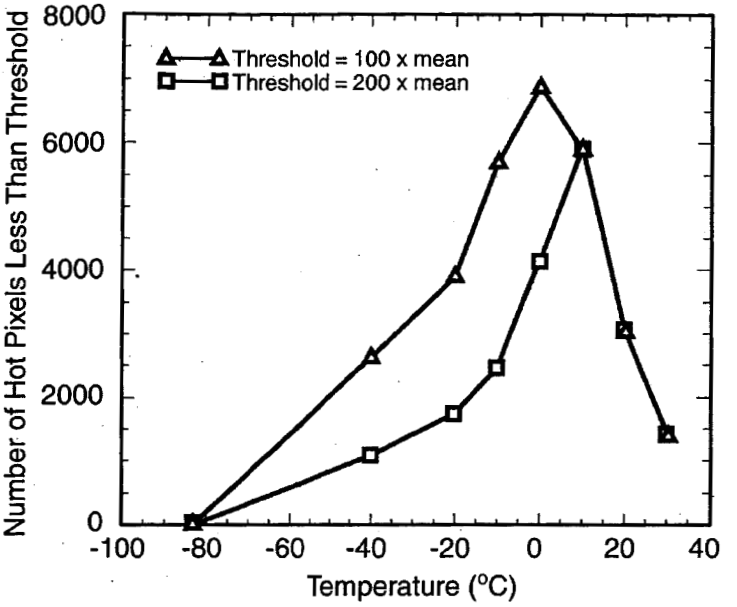

Figure 6. Number of annealed hot pixels versus temperature.

As seen in Figure 7, the dark current distributions at -83°C before and after annealing make it clear that the hot pixels anneal much more effectively than the warmer pixels. It is also true that although the annealed hot pixels may have fallen below the threshold to be a hot pixel, they tend not to rejoin the main distribution but rather retain a dark signal that is higher than most other pixels.

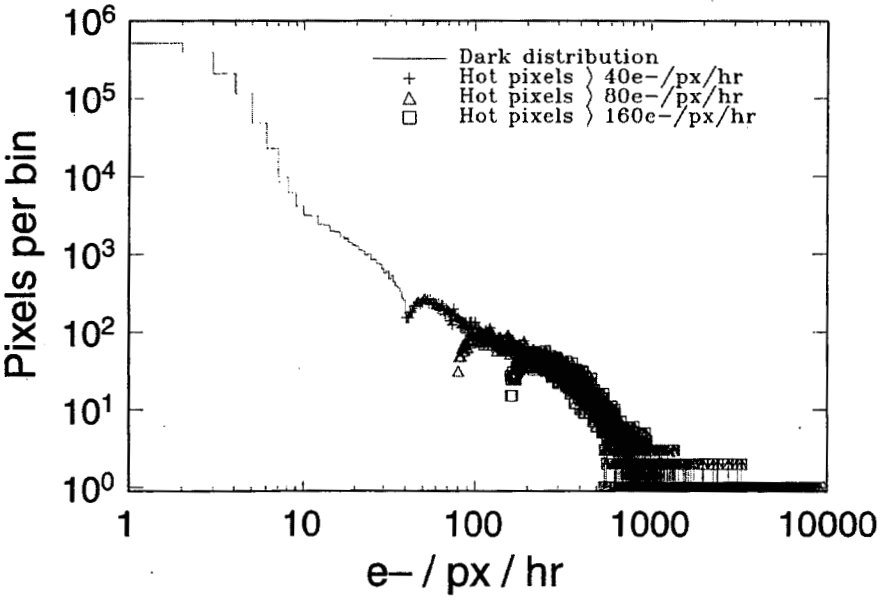

Figure 7a. The distribution of dark signal at -83°C, overplotted with the distributions of the hot pixel populations immediately after irradiation.

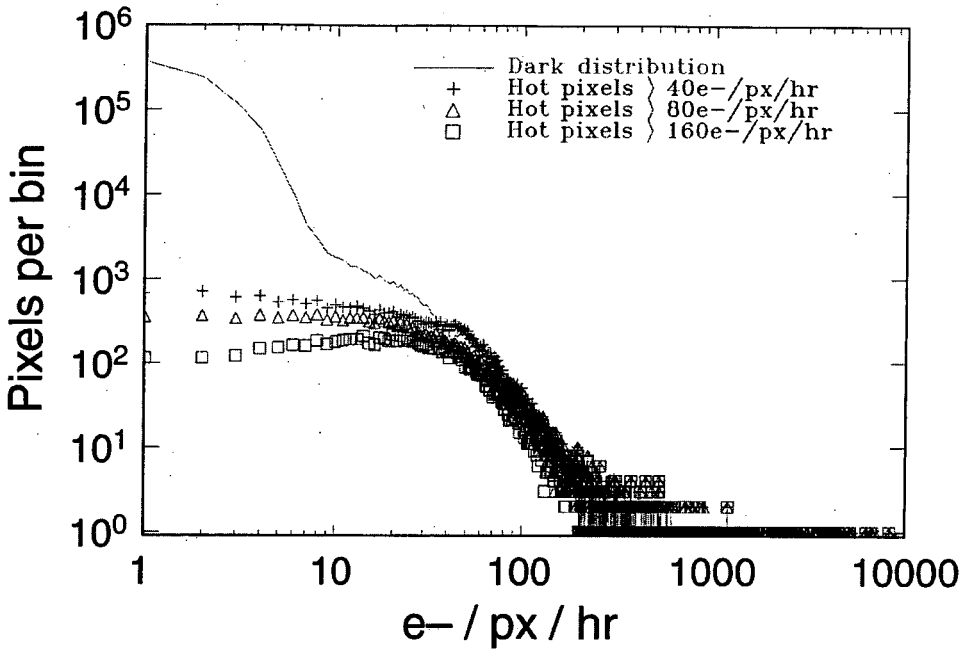

Figure 7b. The distribution of dark signal at -83°C, overplotted with the distributions of the hot pixel populations after annealing at +30°C and cooling back to -83°C.

Finally it is interesting to note that although the dark current annealed significantly on warming from -83°C to +30°C, the charge transfer efficiency did not anneal as expected since the defects responsible (primarily the E-center and divacancy) do not anneal until much higher temperatures. It is not currently known what defects and/or device electric fields are responsible for the dark current annealing characteristics. Further work is planned to examine the dark current activation energies for the hot pixels and compare them to that for the mean pixel population.

SUMMARY

A HST Wide Field Camera 3 (WFC3) E2V CCD was irradiated while operating at -83 °C and the dark current studied as a function of temperature while the CCD was warmed to a sequence of temperatures up to a maximum of +30°C. The device was then cooled back down to -83° and re-measured. Hot pixel populations were tracked during the warm-up and cool-down. Hot pixel annealing began below -40 °C and the anneal process was largely completed before the detector reached +30°C. There was no sharp annealing temperature. Although a large fraction of the hot pixels fell below the threshold to be counted as a hot pixel, they nevertheless remained warmer than the remaining population. The mechanism for the formation and annealing of hot pixels is not presently understood.

ACKNOWLEDGMENTS

The authors appreciate funding from the Wide Field Camera 3 project and the NASA Electronics and Packaging Program (NEPP).

REFERENCES

1. G. R. Hopkinson, C. J. Dale, and P. W. Marshall, "Proton effects in CCDs", IEEE Trans. on Nucl. Sci., Vol. 43, no. 2, pp. 614-627, Apr. 1996.
2. C. Dale, P. Marshall, B. Cummings, L. Shamey and A. Holland, "Displacement damage effects in mixed particle environments for shielded spacecraft CCDs", IEEE Trans. on Nucl. Sci., vol. 40, no. 6, pp. 1628-1637, Dec. 1993.
3. P.W. Marshall, C.J. Dale, and E.A. Burke, "Proton-Induced Displacement Damage Distributions and Extremes in Silicon Microvolumes," IEEE Trans. Nucl. Sci., Vol. 37, No. 6, pp. 1776-1783, 1990.
4. G.R. Hopkinson, "Cobalt-60 and Proton Radiation Effects on Large Format, 2-D, CCD Arrays for an Earth Imaging Application," IEEE Trans. Nucl. Sci., Vol. 39, No. 6, pp. 2018-2025, 1992.
5. J. Bogaerts, B. Dierickx, and R. Mertens, "Enhanced dark current generation in proton-irradiated CMOS active pixel sensors," IEEE Trans. Nucl. Sci., Vol. 99, No. 3, pp. 1513-1521, 2002.
6. M. Clampin, G. Hartig, H.C. Ford, M. Sirianni, G. Meurer, A. Martel, J.P. Blakeslee, G.D. Illingworth, J. Krist, R. Gilliland, and R. Bohlin, "Status for the Advanced Camera for Surveys," 2002 HST Calibration Workshop, Space Telescope Science Institute, October 2002.
7. E.J. Polidan et al., "Hot pixel behavior in WFC3 CCD detectors irradiated under operational conditions," Proc. SPIE 5167, pp. 258-269, 2003.
8. J.R. Srour and D.H. Lo, "Universal Damage Factor for Irradiated-Induced Dark Current in Silicon Devices", IEEE Trans. Nucl. Sci., Vol. 47, No. 6, pp. 2451-2459, 2000.
9. M. Sirianni et al. "Characterization and on-orbit performance of the Advanced Camera for Surveys CCDs, Proc. SPIE 4854, pp. 496-506, 2003
10. R.A. Kimble et al., "Radiation damage effects on the CCD detector of the Space Telescope Imaging Spectrometer," Proc. SPIE 4013, pp. 532-544, 2000.
12. J.R. Srour and R.A. Hartman, "Enhanced Displacement Damage Effectiveness in Irradiated Silicon Devices," IEEE Trans. Nucl. Sci., Vol. 36, No. 6, pp. 1825-1830, 1989.
13. E.J. Polidan et al., "A Study of hot pixel annealing in the Hubble Space Telescope Wide Field Camera 3 CCDs," Proc. SPIE, pp. 289-298, 2004.